Dimerization of Many-Body Subradiant States in Waveguide Quantum Electrodynamics

Alexander V. Poshakinskiy and Alexander N. Poddubny*
Ioffe Institute, St. Petersburg 194021, Russia

(Received 28 June 2021; revised 26 August 2021; accepted 21 September 2021; published 18 October 2021)

We theoretically study subradiant states in an array of atoms coupled to photons propagating in a one-dimensional waveguide focusing on the strongly interacting many-body regime with large excitation fill factor f. We introduce a generalized many-body entropy of entanglement based on exact numerical diagonalization followed by a high-order singular value decomposition. This approach has allowed us to visualize and understand the structure of a many-body quantum state. We reveal the breakdown of fermionized subradiant states with increase of f with the emergence of short-ranged dimerized antiferromagnetic correlations at the critical point $f = 1/2$ and the complete disappearance of subradiant states at $f > 1/2$.

DOI: 10.1103/PhysRevLett.127.173601

Introduction.—The Dicke model, describing collective radiance of dense atomic clouds, is one of the paradigmatic concepts of quantum optics [1,2]. Recently, it has become possible to test the classical ideas of collective spontaneous emission for man-made platforms of waveguide quantum electrodynamics (WQED), studying arrays of natural or artificial atoms (superconducting qubits, quantum dots, quantum defects) coupled to photons propagating in a waveguide [3–5].

Historically, the research has been mainly focused on the superradiant symmetrically excited Dicke states of atomic arrays [6,7]. The subradiant states have attracted attention only recently. Their structure is much more subtle due to intrinsically high spectral degeneracy that can make the spontaneous decay dynamics strongly nonexponential [8,9]. Single-excited ($k = 1$) subradiant states are relatively simple, they can be constructed as a superposition of individual atom excitations that is out of phase with the light wave. The simplest example is a single-excited dark dimer state shown in Fig. 1(a) with the wave function $|\psi\rangle = (\sigma_1^\dagger - \sigma_2^\dagger)|0\rangle/\sqrt{2}$ (here $\sigma_{1,2}^\dagger$ are the atomic raising operators) [10]. Importantly, the smaller is the distance between the atoms d, the darker is the state. The spontaneous decay rate scales as $(d/\lambda_0)^2$ where λ_0 is the wavelength at the atomic resonance. In an atomic array, single-excited dimer states hybridize with each other and form subradiant standing waves [11–17], illustrated in Fig. 1(b). The subradiant states with $k > 1$ excitations have become a subject of active research only relatively recently [8,9,13–19]. In particular, when the excitation fill factor $f = k/N$ is small, subradiant states are antisymmetric products of single-particle subradiant states [14,20], reflecting so-called fermionization of atomic excitations. There also exists an "electron-hole" symmetry between the fill factors f and $1 - f$. Based on such symmetry one can expect interesting effects at the transition point $f = 1 - f = 1/2$ when the excitation degeneracy is at maximum. Indeed, many-body delocalization transition has been predicted in disordered arrays for $f = 1/2$, that can be also naively understood as suppression of disorder by electromagnetically induced transparency (EIT) [21]. Many-body signatures in spontaneous emission cascade for atoms without a waveguide were revealed in [9]. To the best of our knowledge, subradiant multiple excited states in waveguide-coupled atomic arrays have been directly probed only in one very recent experiment with just $N = 4$ superconducting qubits [22]. Moreover, the structure of subradiant states in the strongly many-body regime of $f \sim 1/2$, when the fermionic ansatz [14] is no longer valid, remains unclear.

Here we focus on the subradiant states at large excitation fill factors and demonstrate a strong modification of their lifetimes and spatial structure at the transition point $f = 1/2$. We show that for an array with even atom number N, the darkest subradiant state at $f = 1/2$ is not a simple combination of standing waves, as in Fig. 1(b), but a dimer product state

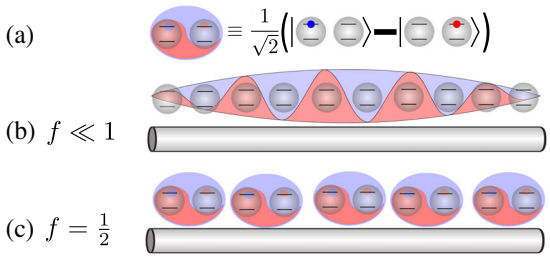

FIG. 1. Schematics of (a) single-excited dimer dark state for two atoms; (b) dark state in array of atoms near a waveguide for small fill factor $f \ll 1$ that is an antisymmetrized product of standing waves [14]; (c) many-body dimerized dark state Eq. (1) for $f = 1/2$.

$$|\psi\rangle = \frac{1}{2^{N/4}}(\sigma_1^\dagger - \sigma_2^\dagger)(\sigma_3^\dagger - \sigma_4^\dagger)\ldots(\sigma_{N-1}^\dagger - \sigma_N^\dagger)|0\rangle, \quad (1)$$

schematically illustrated in Fig. 1(c). The wave function Eq. (1) can be intuitively understood in the following way. First, by construction it is a superposition of $k = N/2$ dark dimer excitations of type Fig. 1(a). Second, we choose only the dimers formed by nearest neighbors, because the smaller the dimer the darker the state. The state Eq. (1) is similar to one predicted in Refs. [23,24], but the setup and the mechanism of dimerization are quite different. In Refs. [23,24], the dimerization results from the driven-dissipative dynamics in a chirally coupled array, when the back-propagation of excitations has been suppressed. Our setup is not chiral and dimerization emerges directly from the structure of subradiant eigenstates, rather than from quantum or nonlinear classical [25,26] dynamics. Our goal is to examine the transformation from the standing waves in Fig. 1(b) to the dimer state Fig. 1(c) with the increase of the fill factor f.

Many-body excitation spectrum.—The structure under consideration is characterized by the following effective Hamiltonian, valid in the usual Markovian and rotating wave approximations [5,19,27], $H = -i\gamma_{1D}\sum_{n,m=1}^{N}\sigma_n^\dagger\sigma_m e^{i\varphi|m-n|}$, where the energy is counted from the atomic resonance $\hbar\omega_0$ and $\varphi = \omega_0 d/c \equiv 2\pi d/\lambda_0$ is the phase gained by light travelling the distance d between two neighboring atoms. The operators $\sigma_m^\dagger$ are the spin 1/2 raising operators, $\sigma_m^2 = 0$, $\sigma_m\sigma_m^\dagger + \sigma_m^\dagger\sigma_m = 1$, $[\sigma_m, \sigma_n] = 0$ for $m \neq n$. The parameter $\gamma_{1D} \equiv \Gamma_{1D}/2$ is the radiative decay rate of single atom into the waveguide, rendering the effective Hamiltonian non-Hermitian. We are interested in the decay rates of multiply excited subradiant eigenstates with k excitations,

$$|\psi^{(k)}\rangle = \sum_{n_1 n_2 \ldots n_k = 1}^{N} \psi_{n_1 n_2 \ldots n_k}\sigma_{n_1}^\dagger\sigma_{n_2}^\dagger\ldots\sigma_{n_k}^\dagger|0\rangle, \quad (2)$$

where the tensor ψ is symmetric and turns to zero if any of the two indices coincide. The decay rates are found numerically from the effective Schrödinger equation $H|\psi^{(k)}\rangle = k\varepsilon|\psi^{(k)}\rangle$ as $\Gamma = -\mathrm{Im}\varepsilon$.

Figures 2(a) and 2(b) present the dependence of the radiative decay rates of most subradiant states on the array period d, and the number of excitations k. The calculated decay rate is the smallest when the period is close to 0 or to $\lambda_0/2$. For $f \ll 1$, it scales as $\Gamma/\gamma_{1D} \sim (d/\lambda_0)^2/N^3$ for $d \to 0$ [14]. When $k \ll N/2$ the most-subradiant multiple-excited states can be approximated by antisymmetric combinations of most subradiant single-excited states with the decay rates $\Gamma_\nu^{(1)}$ [14], $\Gamma^{(k)} = \sum_{\nu=1}^{k}\Gamma_\nu^{(1)}/k$ [black curves in Fig. 2(b)]. However, the situation changes dramatically for $k \geq N/2$, when $f \geq 1/2$. The subradiant states disappear: all the decay rates become larger than those of a single atom, $\Gamma \gtrsim \gamma_{1D}$, in agreement with the qualitative picture in Fig. 1. Such behavior is universal as shown by the phase diagram Fig. 2(c) where we plot the decay rates of most subradiant states for a fixed period depending on both the number of atoms and the number of excitations. Red and blue lines correspond to the fully excited and half-excited arrays, with fill factors $f = 1$ and $f = 1/2$. Clearly, the decay rates in the region between blue and red lines, where $f > 1/2$, are significantly larger than those for $f < 1/2$.

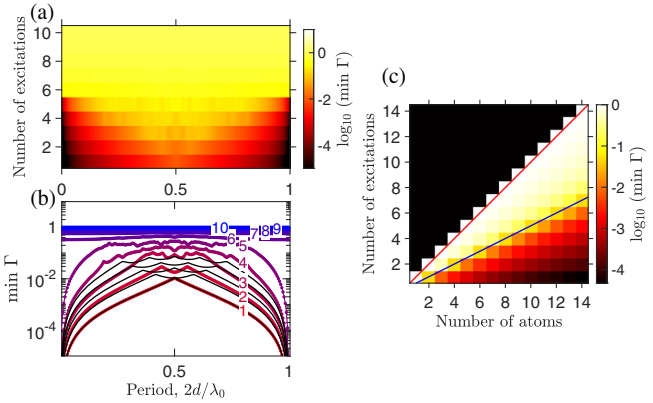

FIG. 2. (a),(b) Dependence of the radiative decay rate $\min\Gamma$ for the most-subradiant state in the 10-atom array on the array period d and number of excitations k. For (b) the number of excitations is shown near each curve. (c) Dependence of $\min\Gamma$ on number of atoms N and number of excitations k calculated for a fixed period $d = 0.05\lambda_0$. Red and blue lines show the dependences $k = N$ (fill factor $f = 1$) and $k = N/2$ ($f = 1/2$), respectively. Decay rates are normalized to γ_{1D}.

The absence of subradiant states for $f > 1/2$ also follows from a general combinatoric argument. The tensor ψ is defined by just C_N^k complex amplitudes due to the permutation symmetry. For subradiant states, these amplitudes satisfy certain linear conditions, that forbid spontaneous decay into all the C_N^{k-1} states with $k-1$ excitations. Thus, the number of k-excited subradiant states is equal to the total number of states minus the number of conditions, $C_N^k - C_N^{k-1}$, and they exist only for $k \leq N/2$. More details, linking multiple-excited states to the states of N spin-1/2 electrons with a certain total momentum, are given in the Supplemental Material [28].

Decompositon of multiple-excited state over single-excited states.—Because of the large size of the Hilbert space, even visualization of the numerically calculated wave function for $k \geq 3$ excitations is quite challenging [20]. However, there exist variational approximations to the full wave function, that represent the full k-rank tensor $\psi_{n_1 n_2 \ldots n_k}$ as a product of several tensors of lower rank, such as matrix product states and tensor network technique [33,34]. Such approaches have already been used in WQED [8,35]. Here, we use a slightly different technique of multilinear singular value decomposition [36,37],

that, contrary to the matrix product state approach, is numerically exact. We represent the k-rank symmetric tensor $\psi_{n_1 n_2 \ldots n_k}$ as

$$\psi_{n_1 n_2 \ldots n_k} = \sum_{\alpha_1 \alpha_2 \ldots \alpha_k = 1}^{N} \Lambda_{\alpha_1 \alpha_2 \ldots \alpha_k} U_{n_1}^{\alpha_1} U_{n_2}^{\alpha_2} \ldots U_{n_k}^{\alpha_k}, \quad (3)$$

where the tensor U is unitary, $\sum_{n=1}^{N} U_n^{\alpha *} U_n^{\alpha'} = \delta_{\alpha \alpha'}$, and the so-called core tensor Λ is symmetric and quasidiagonal, i.e., it satisfies the identity $\sum_{\alpha_2 \ldots \alpha_k = 1}^{N} \Lambda^*_{\alpha_1' \alpha_2 \ldots \alpha_k} \Lambda_{\alpha_1 \alpha_2 \ldots \alpha_k} = 0$ for $\alpha_1 \neq \alpha_1'$. The decomposition Eq. (3) is schematically illustrated in Fig. 3(a). It generalizes the conventional Schmidt (singular) value decomposition of a two-particle wave function (for $k = 2$ one has $\Lambda_{\alpha_1 \alpha_2} \equiv \lambda_{\alpha_1} \delta_{\alpha_1 \alpha_2}$ where λ_α are the usual singular values). In the multilinear decomposition, the role of singular values is played by the Frobenius norms of the subtensor of the tensor Λ defined as [36] $(\lambda_\alpha)^2 = \sum_{\alpha_2 \ldots \alpha_k = 1}^{N} |\Lambda_{\alpha, \alpha_2 \ldots \alpha_k}|^2$. Because of the orthogonality properties of the tensors Λ and U, the sum of $|\psi_{n_1 n_2 \ldots n_k}|^2$ over all the indices is equal just to $\sum_{\alpha=1}^{N} |\lambda_\alpha|^2$, similarly to the case of usual single-particle Schmidt decomposition. This analogy allows us to introduce the generalized entropy of entanglement as

$$S = -\sum_{\alpha=1}^{N} |\lambda_\alpha|^2 \ln |\lambda_\alpha|^2. \quad (4)$$

The expression Eq. (4) has been originally introduced in quantum information theory [38] as a measure of two-particle entanglement. By construction, Eq. (4) is zero for a product state $\psi_{n_1 n_2} = U_{n_1} U_{n_2}$, where only one of $|\lambda_\alpha|^2$ is nonzero and equal to one. Thus, our Eq. (4) quantifies the number of nonzero coefficients $|\lambda_\alpha|^2$, that is a number of product states $U_{n_1}^{\alpha_1} U_{n_2}^{\alpha_2} \ldots U_k^{\alpha_3}$ necessary to describe a general k-excited state ψ. We use the numerical decomposition algorithm from [37] that is numerically efficient only for relatively small $k \ll N$. Thus, for $k > N/2$ it is more instructive to exploit the "electron-hole symmetry" of the problem [8] and represent the k atomic excitations as $N - k$ "holes" in the array of fully excited atoms.

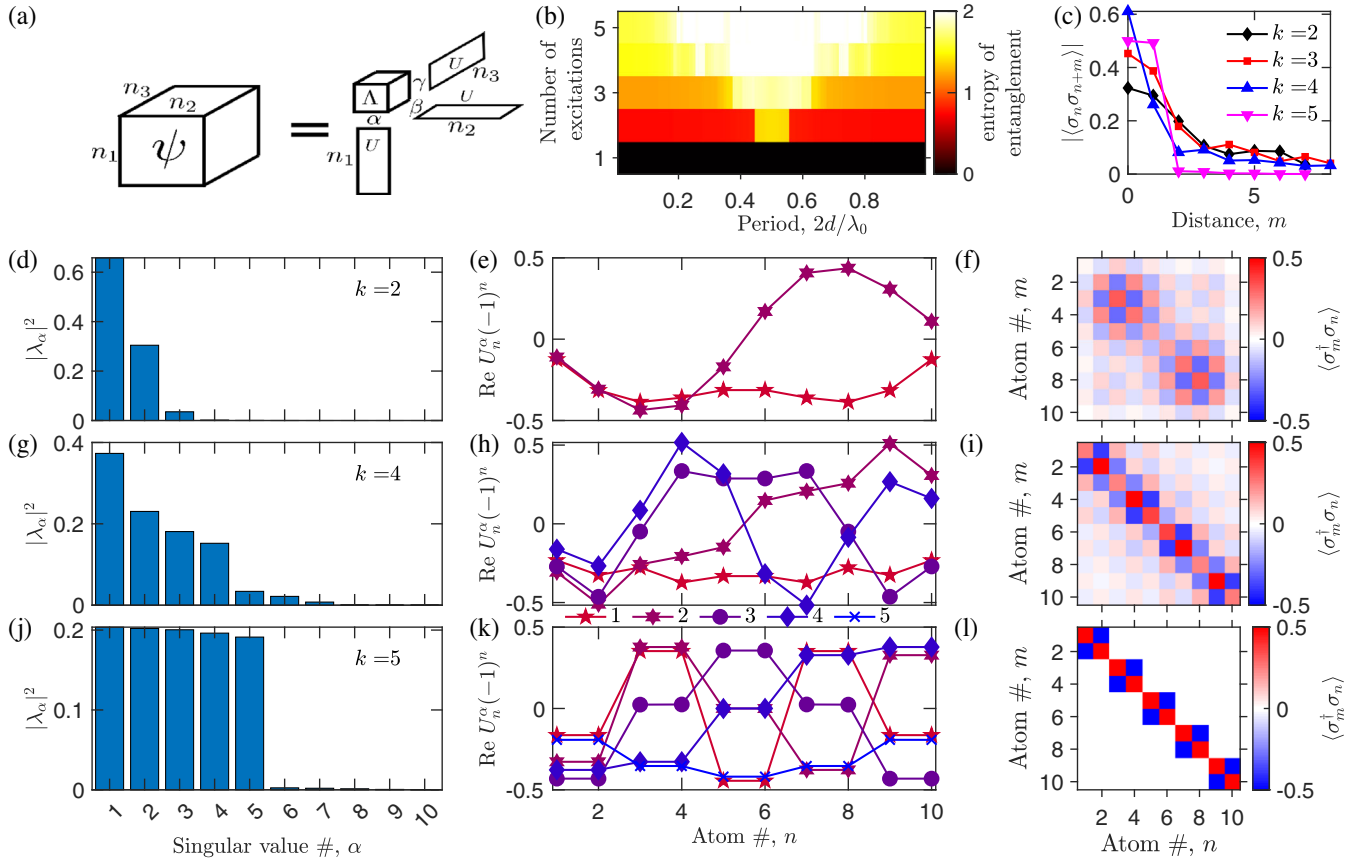

FIG. 3. (a) Illustration of high-order singular value decomposition for a three-particle wave function $\psi_{n_1 n_2 n_3}$. (b) Entanglement entropy Eq. (4) calculated depending on the number of excitations k and the array period d for $N = 10$ atoms. (d)–(l) Distributions of higher order singular values λ_α (left column), eigenvectors U_n^α (middle column), and correlation functions $\langle\sigma_m^\dagger\sigma_n\rangle$ (right column) for the most subradiant states with $k = 2$ (d)–(f), $k = 4$ (g)–(i), and $k = 5$ (j)–(l) excitations. Correlation functions $\langle\sigma_n^\dagger\sigma_{n+m}\rangle$ are also shown in (c) depending on the photon-photon distance m. Calculation has been performed for $d = 0.05\lambda_0$.

The dependence of entanglement entropy of most subradiant states on the number of excitations and the array period is shown in Fig. 3(b). These results are in good qualitative agreement with the radiative decay rates in Fig. 2. The entropy increases, i.e., the states become more complex, for (i) larger numbers of excitations and (ii) stronger detuning of the period d from the degeneracy points $d = 0$ and $d = \lambda_0/2$. We show explicitly all the multilinear singular values in Figs. 3(d), 3(g), and 3(j) depending on the number of excitations. The general observation is that a subradiant state with k excitations has first k multilinear singular values much larger than the remaining $N-k$ ones. This confirms our qualitative interpretation of Eq. (3) as the expansion of a many-body state over single-particle ones. Crucially, the obtained single-particle states U^{α} strongly depend on the number of excitations, i.e., they are renormalized by interactions. When the fill factor is small, as in the case of $f = 1/5$ in Fig. 3(e), the states $U^{1,2}$ are just two standing waves with zero and one node, in agreement with the analytical fermionic ansatz of Ref. [14] for a long array with $d \ll \lambda_0$, see also the Supplemental Material of [19]:

$$U_n^1 \propto (-1)^n \sin\frac{\pi(n-1/2)}{N}, \quad U_n^2 \propto (-1)^n \sin\frac{2\pi(n-1/2)}{N}, \tag{5}$$

$n = 1, 2 \ldots N$. However, the functions U_n^{α} drastically change at the threshold $f = 1/2$, for $k = N/2$ excitations, see Fig. 3(k). Namely, they become "dimerized" with equal amplitudes (up to the sign) at neighboring sites $2k-1$ and $2k$, supporting the naive picture Fig. 1(c). The functions U_n^{α} can be well fitted by the dimerized standing waves

$$U_{2m-1} = -U_{2m} \propto \cos\frac{\pi r(m-\bar{m})}{N} \quad \text{or} \quad \sin\frac{\pi r(m-\bar{m})}{N}, \tag{6}$$

where $m = 0, 1 \ldots N/2$, $\bar{m} = 1/2 + N/4$, and the fit parameters r are given in [28]. The onset of dimerization effect Eq. (6) can be already seen for a double-excited subradiant state in a four-atom array, that reads $|\psi\rangle = \frac{1}{2}(\sigma_1^{\dagger} - \sigma_2^{\dagger})(\sigma_3^{\dagger} - \sigma_4^{\dagger})|0\rangle$ for $d \ll \lambda_0$ [19]. However, since the study in Ref. [19] has been restricted just to the case of just $k = 2$ two excitations, the generality of the dimerization effects was not clear before.

The dimerization of subradiant states is directly visualized by their spin-spin correlation function $\langle \sigma_m^{\dagger}\sigma_n \rangle$, plotted in the right column of Fig. 3. For $k = 2$ excitations the correlations are long-ranged, reflecting the spatial profile of the eigenstates Eq. (5), see Fig. 3(f). At the threshold, for $k = N/2$, the correlations increase and become short-ranged, see Fig. 3(l) and also the cross section in Fig. 3(c). The only significant elements of the correlation matrix at the threshold are $\langle \sigma_m^{\dagger}\sigma_m \rangle \approx \frac{1}{2}$ and $\langle \sigma_{2j-1}^{\dagger}\sigma_{2j} \rangle \approx -\frac{1}{2}$, i.e., there appears a short-range effective antiferromagnetic order.

Detection of the subradiant-to-bright transition.—While single-excited subradiant states can be straightforwardly probed as reflection resonances [39], the optimal protocol to probe multiple-excited subradiant states in an equidistant qubit array is not yet clear because they are weakly coupled to the waveguide. Qubits or atoms should be probably excited locally from the side and the spin-spin correlation functions can be then measured also locally. However, interesting results can be potentially obtained even from the incoherent scattering spectra measured directly through the waveguide. We assume that the array is coherently excited from the left at the frequency ω, as described by the coupling term $\sqrt{P\gamma_{1D}}\sum_{j=1}^{N}(\sigma_j e^{-i(\omega-\omega_0)t} + \text{H.c.})$ in the electric dipole and rotating wave approximations, where P is the normalized input power. Next, we use the input-output theory [40] and calculate the total amount of incoherently scattered photons $I(\omega) = 1 - |r(\omega)|^2 - |t(\omega)|^2$, where $r(\omega)$ and $t(\omega)$ are the amplitudes of coherent reflection and transmission coefficients. Incoherent scattering spectra calculated for a 4-atom array are shown in Fig. 4(a). At low power, the spectra show narrow peaks centered at the frequencies of the single-excited subradiant states, shown by vertical dashes at the bottom horizontal axis in Fig. 4(a). At higher powers, these peaks shift and broaden, making it quite hard to identify possible manifestation of double excited states (vertical dashes at the top horizontal axis). The peak corresponding to the most subradiant double-excited state at $(\omega-\omega_0)/\gamma_{1D} \approx -0.3$ is definitely not resolved. However, a second peak $(\omega-\omega_0)/\gamma_{1D} \approx -0.7$, seen at higher powers (dark red curve) could be related to a second double-excited subradiant state. We have also extracted

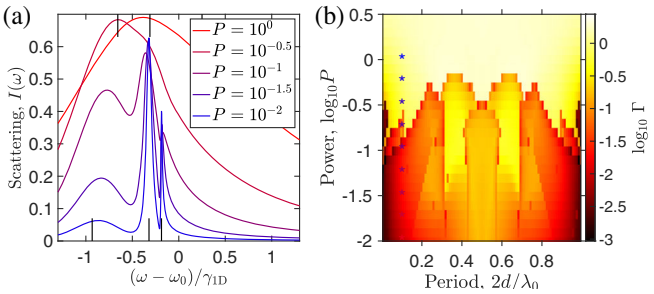

FIG. 4. (a) Incoherent scattering spectra calculated for an array of $N = 4$ atoms with the period $d = 0.05\lambda_0$ for several powers indicated on graph. Vertical dashes at the bottom (upper) horizontal axis show the frequencies of the two most subradiant states with $k = 1$ ($k = 2$) excitations, respectively. (b) Linewidth of the narrowest resonance feature in the incoherent scattering spectra depending on the pump power P and the array period. Stars in (b) indicate the values of parameters used for calculation in (a). The excitation power has been normalized to γ_{1D}.

from each spectrum the linewidth of the narrowest peak and plotted it by color in Fig. 4(b) as a function the pump power P and the array period. The result qualitatively resembles Fig. 2(a): narrow spectral features, corresponding to subradiant states, become wider with the power increase and disappear above a certain threshold. Similarly to Fig. 2(a), an interesting nonmonotonous behavior is observed near the anti-Bragg period $d = \lambda_0/4$. However, in the considered setup all the occupation numbers $\langle \sigma_m^\dagger \sigma_m \rangle$ stay below $1/2$ and the threshold $f = 1/2$ is never crossed. Nevertheless, the evolution of the incoherent scattering spectra with pump power similar to Fig. 4 could be an important precursor of the subradiant-to-bright transition.

Outlook.—Our findings provide yet another demonstration of the fundamental many-body physics in the waveguide quantum electrodynamics setup. In this work, we have limited ourselves to relatively short arrays with just $N \lesssim 10$ atoms, that are well within the range of state-of-the-art experimental structures with superconducting qubits [41]. We expect much richer physics for larger arrays, when bound photon pairs start playing a role [42]. For example, it is quite intriguing whether "magic periods" such as $d = \lambda_0/12$ [43,44] with a quasiflat band of composite excitations survive in the many-body regime. Another standing problem is the influence of disorder and the possible interplay of the many-body delocalization transition [21] with the subradiant-to-bright transition for $f = 1/2$ fill factor. On the more applied side, our results could be useful to design long-living complex quantum correlations.

The authors are grateful to M. M. Glazov and M. O. Nestoklon for useful discussions. This work has been funded by the Russian President Grant No. MD-243.2020.2. A. V. P. also acknowledges support by the Theoretical Physics and Mathematics Advancement Foundation "BASIS."

*poddubny@coherent.ioffe.ru

[1] R. H. Dicke, Coherence in spontaneous radiation processes, Phys. Rev. **93**, 99 (1954).
[2] M. O. Scully and A. A. Svidzinsky, The super of superradiance, Science **325**, 1510 (2009).
[3] D. Roy, C. M. Wilson, and O. Firstenberg, Colloquium: Strongly interacting photons in one-dimensional continuum, Rev. Mod. Phys. **89**, 021001 (2017).
[4] D. E. Chang, J. S. Douglas, A. González-Tudela, C.-L. Hung, and H. J. Kimble, Colloquium: Quantum matter built from nanoscopic lattices of atoms and photons, Rev. Mod. Phys. **90**, 031002 (2018).
[5] A. S. Sheremet, M. I. Petrov, I. V. Iorsh, A. V. Poshakinskiy, and A. N. Poddubny, Waveguide quantum electrodynamics: Collective radiance and photon-photon correlations, arXiv:2103.06824.
[6] J. C. MacGillivray and M. S. Feld, Theory of superradiance in an extended, optically thick medium, Phys. Rev. A **14**, 1169 (1976).
[7] V. Yudson and V. Rupasov, Exact Dicke superradiance theory: Bethe wavefunctions in the discrete atom model, Sov. Phys. JETP **59**, 478 (1984), http://jetp.ras.ru/cgi-bin/e/index/e/59/3/p478?a=list.
[8] L. Henriet, J. S. Douglas, D. E. Chang, and A. Albrecht, Critical open-system dynamics in a one-dimensional optical-lattice clock, Phys. Rev. A **99**, 023802 (2019).
[9] S. J. Masson, I. Ferrier-Barbut, L. A. Orozco, A. Browaeys, and A. Asenjo-Garcia, Many-Body Signatures of Collective Decay in Atomic Chains, Phys. Rev. Lett. **125**, 263601 (2020).
[10] R. G. DeVoe and R. G. Brewer, Observation of Superradiant and Subradiant Spontaneous Emission of Two Trapped Ions, Phys. Rev. Lett. **76**, 2049 (1996).
[11] M. R. Vladimirova, E. L. Ivchenko, and A. V. Kavokin, Exciton polaritons in long-period quantum-well structures, Semiconductors **32**, 90 (1998).
[12] W. Guerin, M. O. Araújo, and R. Kaiser, Subradiance in a Large Cloud of Cold Atoms, Phys. Rev. Lett. **116**, 083601 (2016).
[13] D. F. Kornovan, N. V. Corzo, J. Laurat, and A. S. Sheremet, Extremely subradiant states in a periodic one-dimensional atomic array, Phys. Rev. A **100**, 063832 (2019).
[14] Y.-X. Zhang and K. Mølmer, Theory of Subradiant States of a One-Dimensional Two-Level Atom Chain, Phys. Rev. Lett. **122**, 203605 (2019).
[15] A. Albrecht, L. Henriet, A. Asenjo-Garcia, P. B. Dieterle, O. Painter, and D. E. Chang, Subradiant states of quantum bits coupled to a one-dimensional waveguide, New J. Phys. **21**, 025003 (2019).
[16] J. Rui, D. Wei, A. Rubio-Abadal, S. Hollerith, J. Zeiher, D. M. Stamper-Kurn, C. Gross, and I. Bloch, A subradiant optical mirror formed by a single structured atomic layer, Nature (London) **583**, 369 (2020).
[17] K. E. Ballantine and J. Ruostekoski, Subradiance-protected excitation spreading in the generation of collimated photon emission from an atomic array, Phys. Rev. Research **2**, 023086 (2020).
[18] A. Asenjo-Garcia, M. Moreno-Cardoner, A. Albrecht, H. J. Kimble, and D. E. Chang, Exponential Improvement in Photon Storage Fidelities using Subradiance and Selective Radiance in Atomic Arrays, Phys. Rev. X **7**, 031024 (2017).
[19] Y. Ke, A. V. Poshakinskiy, C. Lee, Y. S. Kivshar, and A. N. Poddubny, Inelastic Scattering of Photon Pairs in Qubit Arrays with Subradiant States, Phys. Rev. Lett. **123**, 253601 (2019).
[20] J. Zhong and A. N. Poddubny, Classification of three-photon states in waveguide quantum electrodynamics, Phys. Rev. A **103**, 023720 (2021).
[21] N. Fayard, L. Henriet, A. Asenjo-Garcia, and D. Chang, Many-body localization in waveguide QED, Phys. Rev. Research **3**, 033233 (2021).
[22] M. Zanner, T. Orell, C. M. F. Schneider, R. Albert, S. Oleschko, M. L. Juan, M. Silveri, and G. Kirchmair, Coherent control of a symmetry-engineered multi-qubit

dark state in waveguide quantum electrodynamics, arXiv:2106.05623.
[23] T. Ramos, H. Pichler, A. J. Daley, and P. Zoller, Quantum Spin Dimers from Chiral Dissipation in Cold-Atom Chains, Phys. Rev. Lett. **113**, 237203 (2014).
[24] H. Pichler, T. Ramos, A. J. Daley, and P. Zoller, Quantum optics of chiral spin networks, Phys. Rev. A **91**, 042116 (2015).
[25] L. Zhang, W. Xie, J. Wang, A. Poddubny, J. Lu, Y. Wang, J. Gu, W. Liu, D. Xu, X. Shen, Y. G. Rubo, B. L. Altshuler, A. V. Kavokin, and Z. Chen, Weak lasing in one-dimensional polariton superlattices, Proc. Natl. Acad. Sci. U.S.A. **112**, E1516 (2015).
[26] A. V. Nalitov, T. C. H. Liew, A. V. Kavokin, B. L. Altshuler, and Y. G. Rubo, Spontaneous Polariton Currents in Periodic Lateral Chains, Phys. Rev. Lett. **119**, 067406 (2017).
[27] T. Caneva, M. T. Manzoni, T. Shi, J. S. Douglas, J. I. Cirac, and D. E. Chang, Quantum dynamics of propagating photons with strong interactions: A generalized input–output formalism, New J. Phys. **17**, 113001 (2015).
[28] See Supplemental Material at http://link.aps.org/supplemental/10.1103/PhysRevLett.127.173601 for results of auxiliary calculations and theoretical details, which includes Refs. [29–32].
[29] R. Pauncz, *The Construction of Spin Eigenfunctions: An Exercise Book* (Springer Science & Business Media, New York, 2012).
[30] H. Weyl, G. Rumer, and E. Teller, Eine für die Valenztheorie geeignete Basis der binären Vektorinvarianten, Göttingen Nachr. **1932**, 499 (1932), https://eudml.org/doc/59396.
[31] L. Pauling, The calculation of matrix elements for Lewis electronic structures of molecules, J. Chem. Phys. **1**, 280 (1933).
[32] M. Simonetta, E. Gianinetti, and I. Vandoni, Valence-bond theory for simple hydrocarbon molecules, radicals, and ions, J. Chem. Phys. **48**, 1579 (1968).
[33] U. Schollwöck, The density-matrix renormalization group in the age of matrix product states, Ann. Phys. (Amsterdam) **326**, 96 (2011).
[34] R. Orús, A practical introduction to tensor networks: Matrix product states and projected entangled pair states, Ann. Phys. (Amsterdam) **349**, 117 (2014).
[35] S. Arranz Regidor, G. Crowder, H. Carmichael, and S. Hughes, Modeling quantum light-matter interactions in waveguide QED with retardation, nonlinear interactions, and a time-delayed feedback: Matrix product states versus a space-discretized waveguide model, Phys. Rev. Research **3**, 023030 (2021).
[36] L. D. Lathauwer, B. D. Moor, and J. Vandewalle, A multilinear singular value decomposition, SIAM J. Matrix Anal. Appl. **21**, 1253 (2000).
[37] N. Vervliet, O. Debals, L. Sorber, M. Van Barel, and L. De Lathauwer, Tensorlab 3.0 (2016), https://www.tensorlab.net, available online.
[38] J. Eisert, M. Cramer, and M. B. Plenio, Colloquium: Area laws for the entanglement entropy, Rev. Mod. Phys. **82**, 277 (2010).
[39] J. D. Brehm, A. N. Poddubny, A. Stehli, T. Wolz, H. Rotzinger, and A. V. Ustinov, Waveguide bandgap engineering with an array of superconducting qubits, npj Quantum Mater. **6**, 10 (2021).
[40] K. Lalumière, B. C. Sanders, A. F. van Loo, A. Fedorov, A. Wallraff, and A. Blais, Input-output theory for waveguide QED with an ensemble of inhomogeneous atoms, Phys. Rev. A **88**, 043806 (2013).
[41] Y. Ye *et al.*, Propagation and Localization of Collective Excitations on a 24-Qubit Superconducting Processor, Phys. Rev. Lett. **123**, 050502 (2019).
[42] Y.-X. Zhang, C. Yu, and K. Mølmer, Subradiant bound dimer excited states of emitter chains coupled to a one dimensional waveguide, Phys. Rev. Research **2**, 013173 (2020).
[43] A. N. Poddubny, Quasiflat band enabling subradiant two-photon bound states, Phys. Rev. A **101**, 043845 (2020).
[44] Y.-X. Zhang and K. Mølmer, Subradiant Emission from Regular Atomic Arrays: Universal Scaling of Decay Rates from the Generalized Bloch Theorem, Phys. Rev. Lett. **125**, 253601 (2020).